NASA CR-787

A LABORATORY MEASUREMENT OF METEOR LUMINOUS EFFICIENCY

By J. F. Friichtenicht, J. C. Slattery, and E. Tagliaferri

Prepared under Contract No. NASw-1336 by
TRW SYSTEMS
Redondo Beach, Calif.

for

NATIONAL AERONAUTICS AND SPACE ADMINISTRATION

For sale by the Clearinghouse for Federal Scientific and Technical Information
Springfield, Virginia 22151 – CFSTI price $3.00

A LABORATORY MEASUREMENT OF METEOR LUMINOUS EFFICIENCY*

by J. F. Friichtenicht, J. C. Slattery, and E. Tagliaferri

ABSTRACT

The luminous efficiency τ_x, as defined in meteor theory, has been determined by measuring the total radiant energy from luminous trails produced by injecting high velocity, sub-micron diameter, iron particles into gaseous targets. The high velocity particles were obtained from an electrostatic particle accelerator and the velocity and mass of each particle was measured prior to entering the gas. Particle velocities ranged from about 15 km/sec to 40 km/sec. In this velocity range, the particles are completely vaporized while suffering small deceleration, which is also the case for most natural meteors. The total radiant energy from the trail was determined by means of a calibrated photomultiplier tube.

The luminous efficiency in the spectral band 3400-6300 A for an air target and iron particles was found to be nearly constant over the velocity interval from 20 to 40 km/sec. This is in agreement with the theoretical treatment of Öpik for meteors with greatly diluted comas. However, the average value of τ_x was about 0.005 which is about two or three times larger than Öpik's predicted value. At 20 km/sec the results are in good agreement with the value given recently by Verniani. However, Verniani's results indicate a linear velocity dependence. Hence the agreement deteriorates at higher velocities.

*Supported by NASA under Contract NASw-1336.

A LABORATORY MEASUREMENT OF METEOR LUMINOUS EFFICIENCY

by J. F. Friichtenicht, J. C. Slattery, and E. Tagliaferri

1. INTRODUCTION

The quantity meteor luminous efficiency τ_s is defined by the expression

$$I_s = -\frac{1}{2}\tau_s v^2 \, dm/dt \qquad (1)$$

where I_s is the instantaneous luminous intensity of the meteor trail in the spectral range s, m and v are the mass and velocity of the meteoroid, and dm/dt is the rate of mass loss of the meteoroid. It is generally assumed that the primary mechanism of mass loss is by evaporation of atoms from the meteoroid surface and that the luminous trail arises from the de-excitation of collisionally excited meteor atoms and air molecules (or atoms). For high initial velocities, the kinetic energy per meteor atom is large enough to ensure total meteoroid vaporization while it suffers negligible deceleration. For this special case, Eq. (1) can be integrated directly yielding

$$E_s = \tau_s \frac{1}{2} m_o v_o^2 = \tau_s E_o \qquad (2)$$

where E_s is the total radiant energy from the meteor trail in the spectral range s and E_o is the kinetic energy of the meteoroid before it enters the atmosphere.

As expressed in Eq. (2), τ_s is dimensionless and simply represents the fraction of meteor kinetic energy converted to radiant energy.

Astronomers traditionally express meteor intensity in terms of photographic or visual magnitudes and the value (and dimensions) of τ_s must be adjusted accordingly. Throughout this report, we use τ_s as given in Eq. (2) and we denote the experimentally measured luminous efficiency by τ_x.

In order to deduce the meteor mass from photographic records of the trails, τ_s must be known. At present, τ_s is not known with a high degree of confidence. This stems from the complexity of the atomic collision processes involved. In the general case, the meteoroid is composed of a number of different atomic species and they all interact with atmospheric molecules. Add to this the fact that each atom suffers multiple collisions before reaching equilibrium with the atmosphere and it can be seen that the number of possible excited levels becomes enormous.

Numerous attempts utilizing several different approaches have been made to solve this problem. These range from the analytical approach of Öpik[1] to the use of rockets to produce artificial meteors in the earth's atmosphere as described, for example, by McCrosky and Soberman,[2] Jewell and Wineman,[3] and Ayers.[4] Verniani[5] determined the ratio of luminous efficiency to meteor density for a number of photographic meteors and, by then assuming a value for the density, obtained values for the luminous efficiency. Both Verniani's paper and a recent review article by Romig[6] contain extensive bibliographies pertaining to the general problem of determining meteor luminous efficiency.

In this paper, we describe an attempt to determine τ_s by a laboratory measurement. The experiments are implemented by injecting high velocity, sub-micron diameter, solid iron particles into low pressure gas targets and measuring the total luminous energy emitted from the trail as the particle vaporizes in the gas. The mechanism of producing the luminous trail in the laboratory experiments is the same as that for naturally occurring meteors. Furthermore, the particle material, iron, is one of the more important elements found in meteorites. The main differences between these experiments and natural meteor phenomena are the size of the particle and the absolute gas pressure in the target chamber. Since the luminous trail arises from reactions on an atomic scale, the difference in particle size appears

to be of no consequence. The effect of higher gas pressure is more difficult to assess. Natural meteors occur at altitudes where the mean free path is such that collisionally excited atoms or molecules probably de-excite before suffering additional collisions. This may not be the case for the laboratory experiments where the probability of collisions between excited atoms is increased because of the higher gas pressure. It is conceivable that a systematic error in the measured luminous efficiency could be introduced by this effect. Additional analytical and experimental work will be required in order to fully evaluate the applicability of these experiments to the observation of natural meteors.

2. EXPERIMENTAL TECHNIQUES AND PROCEDURES

2.1 TOTAL LUMINOSITY MEASUREMENT

The techniques utilized in these experiments are quite similar to those described by Slattery and Friichtenicht[7] in their paper on ionizing probabilities and only a brief review will be given here. A sketch of the experimental apparatus is shown in Figure 1. The high velocity iron particles are obtained from an electrostatic particle accelerator[8] which consists principally of a 2-million-volt Van de Graaff generator and a charged particle injector. The velocity v_o and charge q of each particle used in the experiment are determined by means of detectors which have been described elsewhere.[9,10] The output signal from one of these detectors is a rectangular voltage pulse, the amplitude of which is proportional to the particle charge while the duration gives the particle transit time through the detector. Although the particle velocity can be obtained from a single detector, the accuracy is improved by measuring the transit time of the particle between two detectors placed a large distance ($\sim$ 100 cm) apart. This is accomplished by triggering the sweep of an oscilloscope by the signal from the first detector. The signal from the second detector is displayed on this sweep and the time interval between the start of the trace and the leading edge of the signal from the second detector gives the transit time between the two detectors. The particle charge q is proportional to the amplitude of the

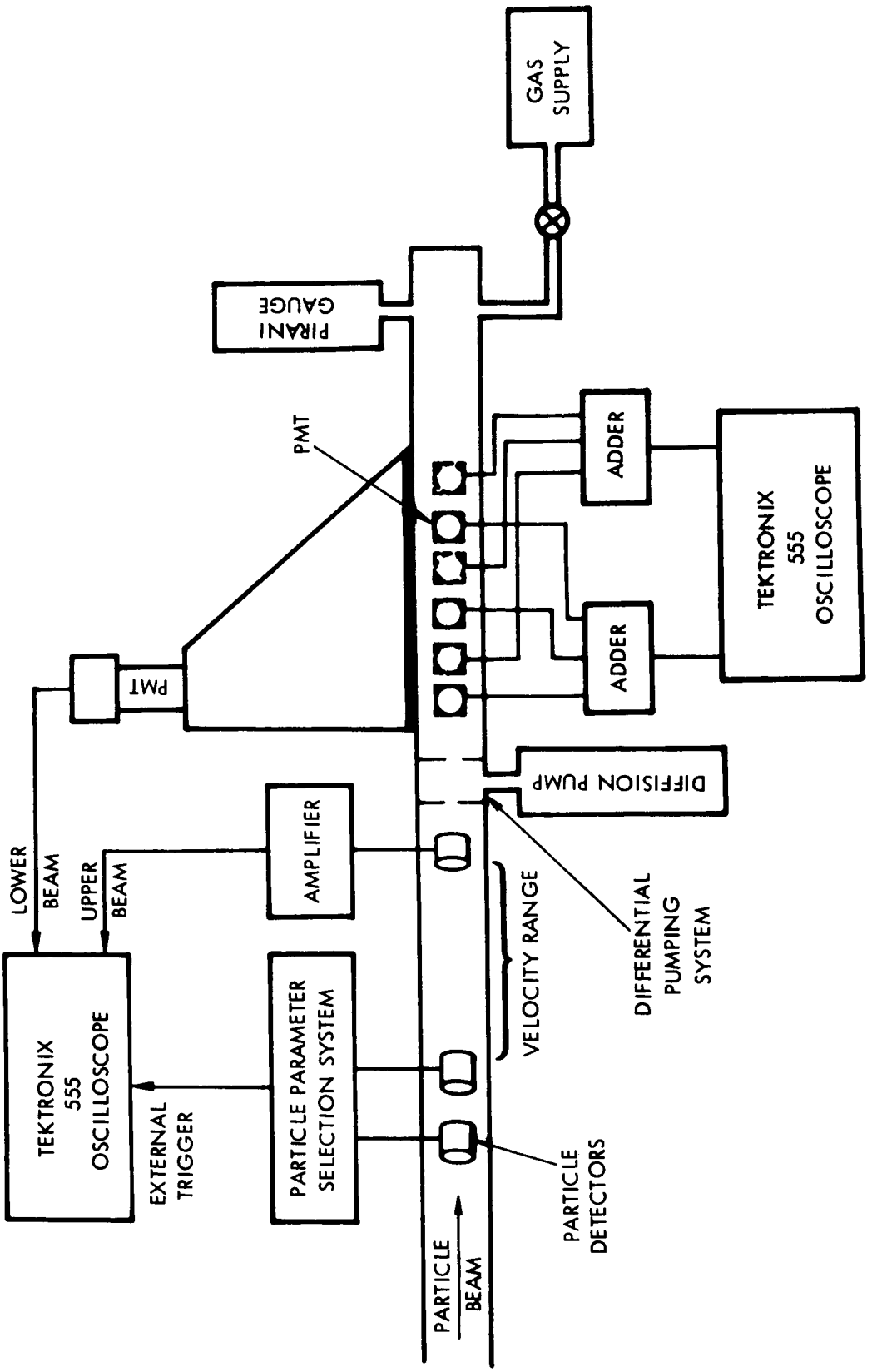

Figure 1. Schematic Diagram of the Experimental Apparatus.

signal from the second detector.

Given v_o and q, the particle mass m_o is calculated from $1/2\ mv_o^2 = qV$ where V is the total accelerating voltage of the Van de Graaff generator.

Only a small fraction of the total flux of particles from the accelerator is compatible with a given set of experimental conditions. Because of the method of charging, the particle velocity is a function of mass, and an adequate selection of satisfactory particles can be made by requiring that the particle velocity lie in some predetermined interval. This is accomplished by the particle parameter selector shown in Figure 1. This device permits selected particles to enter the experiment while automatically rejecting all others. One of the particle detectors used in this unit also provides the trigger pulse which starts the oscilloscope sweep.

After traversing the velocity measuring range, the particles enter the gas target region by passing through the isolating channels of a one-stage differential pumping system. The channels are 0.100 inch diameter by 1 cm long and a pressure of several tenths Torr can be supported in the target chamber without appreciably affecting the main accelerator vacuum which is nominally 10^{-5} Torr. The pressure in the target chamber is adjusted by means of a precision variable leak control and is continuously monitored with a Pirani gauge. The correct pressure to be used is fixed by the requirement that the particle be completely vaporized while within the confines of the target chamber and was determined by trial and error for different ranges of particle velocities.

Upon entering the target gas, the particle is heated to the vaporization point by collisions with the target gas molecules. The remaining mass of a particle which enters the gas with a velocity v_o and decelerates to a lower velocity v is given by

$$m = m_o\, e^{-\frac{\lambda}{4\Gamma\zeta}(v_o^2 - v^2)}\ , \qquad (3)$$

where λ, Γ, and ζ are, respectively, the heat transfer coefficient, the

drag coefficient, and the latent heat of vaporization. Choosing representative values for λ, Γ, and ζ, it can be shown that $m = .01\ m_o$ for a particle decelerated from an initial velocity of 40 km/sec to a final velocity of 38.4 km/sec. In other words, for high initial velocities, the particle is almost completely vaporized while suffering negligible (or at least small) deceleration. It should be noted that the preceding expression is valid regardless of the magnitude of the particle mass. However, the range of a particle in the gas is mass dependent and the pressure in the chamber must be adjusted to insure that the particle vaporizes entirely while still in the target chamber. For small deceleration $v_o \approx v_f$ and we take $1/2\ m_o v_o^2$ as the kinetic energy available for producing radiant energy.

The total radiant energy emitted from the vaporizing particle was determined by means of a calibrated RCA 6199 photomultiplier tube (PMT). The PMT was positioned with its axis perpendicular to the axis of the particle beam and at a distance of 30 cm from the nominal center of the beam axis. The axis of the PMT was located $\sim$ 4 cm downstream from the entrance aperture of the target chamber. A one-inch wide slot, which extended the full length of the target chamber ($\sim$ 31 cm), served as the viewing port. In addition to the main PMT, six other PMT's (three on either side of the target chamber) were positioned along the length of the target chamber. These gave a measure of the length of the luminous trail.

The PMT bases were wired in a conventional manner with the photocathode at a negative high voltage and the anode at ground. The current from the main PMT was effectively integrated at the anode by installing a small capacitor in parallel with a large anode resistor. The RC time constant at the anode was fixed at $\sim$ 10 msec which was very long compared to the time interval over which radiation was emitted. Thus, the voltage amplitude of the pulse appearing at the anode of the PMT was proportional to the total radiant energy produced by the vaporizing particles. In contrast to this, the other six PMT's were sensitive to instantaneous luminous intensity. The output signals from all of the PMT's were fed to broad-band emitter follower circuits and then to the appropriate recording oscilloscopes.

The solid angle subtended by the photocathode of the main PMT is a

function of position along the axis of the particle beam as is the instantaneous intensity of the trail. The total radiant energy incident on the photocathode is given by $\int I(x)\ \Omega(x)\ dx$ where $I(x)$ is the intensity and $\Omega(x)$ is the subtended solid angle at each point along the trail. By assuming constant particle velocity, the intensity variation as a function of position can be determined by the use of Eq. (1) providing the end point of the trail is specified. The end point of the trail was identified for each particle by means of the 6 PMT's stationed along the trajectory of the particle. It was assumed that the luminous trail ended at the position of the PMT which did not give a detectable output signal. The integral was evaluated for each of the six possible end points and a suitable correction was made to the measured pulse height from the PMT to account for these effects. The extreme values of the correction factor differed by only about 10% so the inability to specify precisely the end point of the luminous trail does not introduce an appreciable error in the final results.

In summary, for each experimental event photographic records were made from which particle mass and velocity, the radiant energy incident on the main PMT, and the length of the luminous trail could be obtained. The various pulse amplitudes and time intervals were measured to four-figure accuracy by means of a Tele-reader projector. Following reduction of the raw data, an appropriate correction was made to the radiant energy measurement to account for differences in trail length.

2.2 RESULTS OF TOTAL LUMINOSITY MEASUREMENTS

The data obtained from this set of experiments are shown graphically in Figures 2 through 5 for target gases of air, nitrogen, oxygen, and argon. Here, the quantity Q/m_o is plotted as a function of the initial particle velocity for each particle. Q represents the integrated current that would be measured at the anode of the PMT if all of the radiation from the trail was incident on the photocathode of the tube and is obtained by multiplying the measured charge by an appropriate solid angle correction factor.

It can be seen that Q is a measure of the luminous energy emanating from the trail. However, the measured charge does not uniquely define the

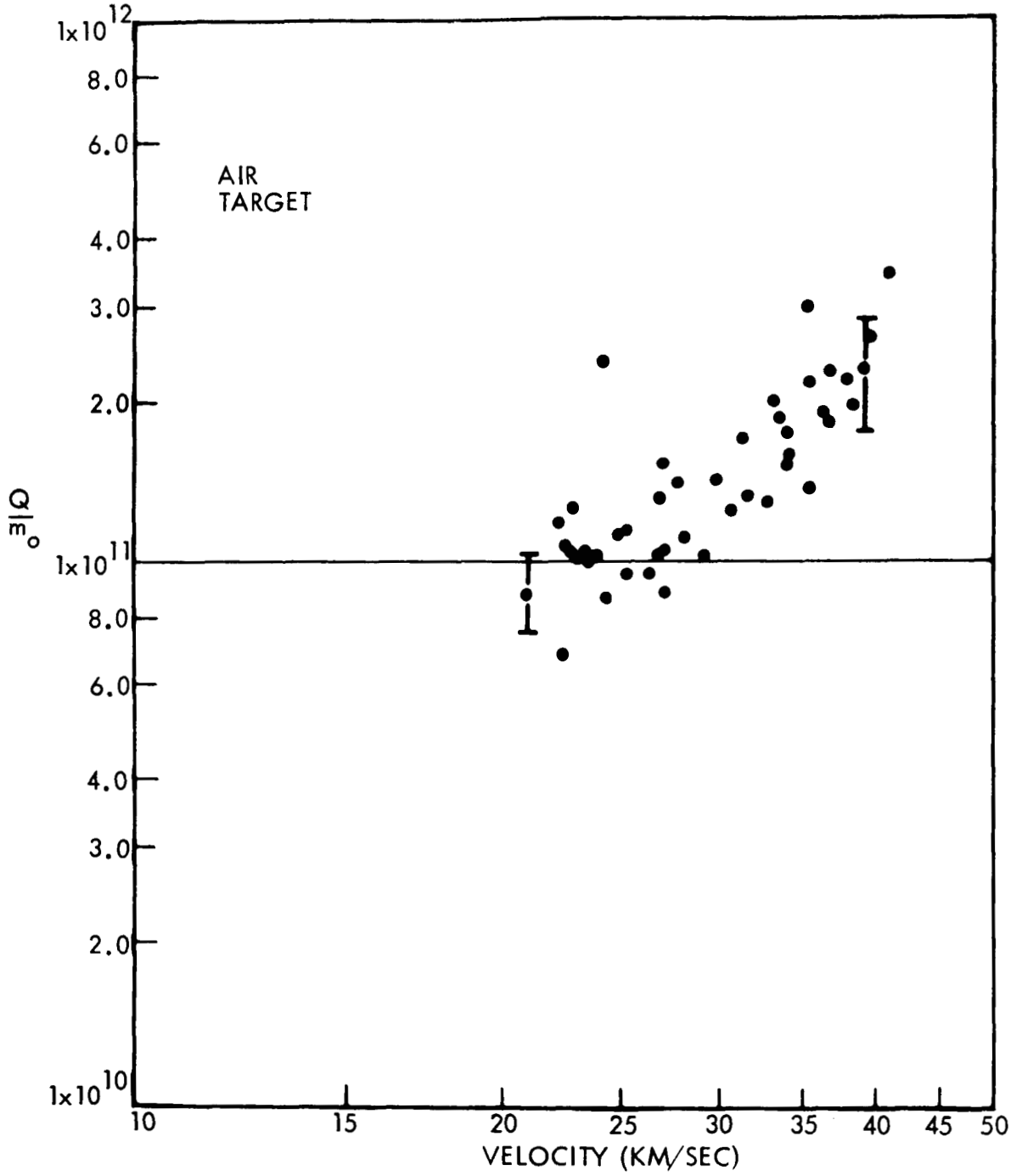

Figure 2. The quantity Q/m_o as a function of velocity for iron particles and an <u>air</u> target gas. m_o is the particle mass and Q is the integrated current at the anode of an RCA 6199 PMT corrected for 100% light collection efficiency. The radiant sensitivity of the PMT was $7.8 \pm 1.8 \times 10^4$ amperes/joule. The error bars indicate the magnitude of the estimated random errors.

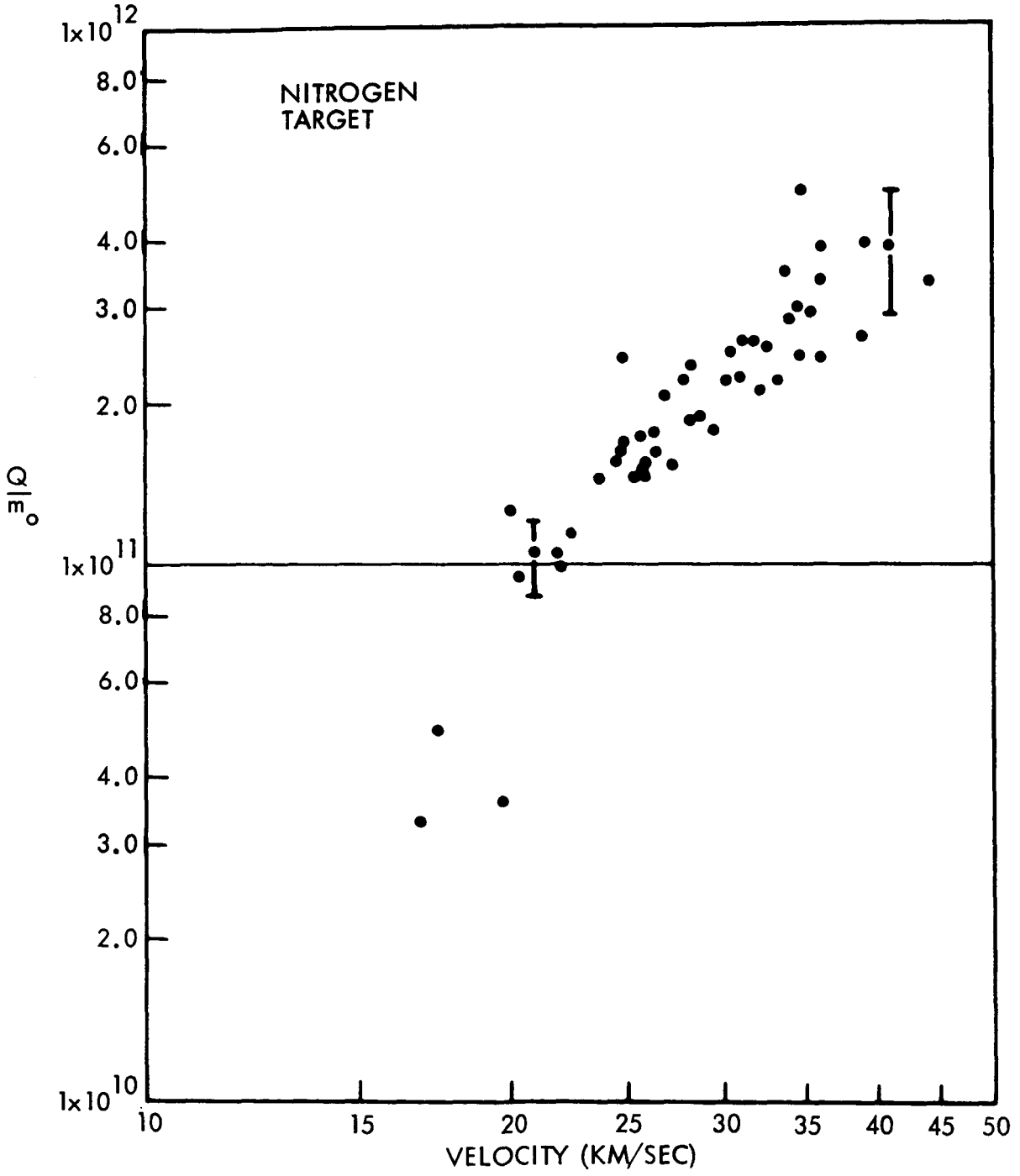

Figure 3. The quantity Q/m_o as a function of velocity for iron particles and a nitrogen target gas. m_o is the particle mass and Q is the integrated current at the anode of an RCA 6199 PMT corrected for 100% light collection efficiency. The radiant sensitivity of the PMT was $7.8 \pm 1.8 \times 10^4$ amperes/joule. The error bars indicate the magnitude of the estimated random errors.

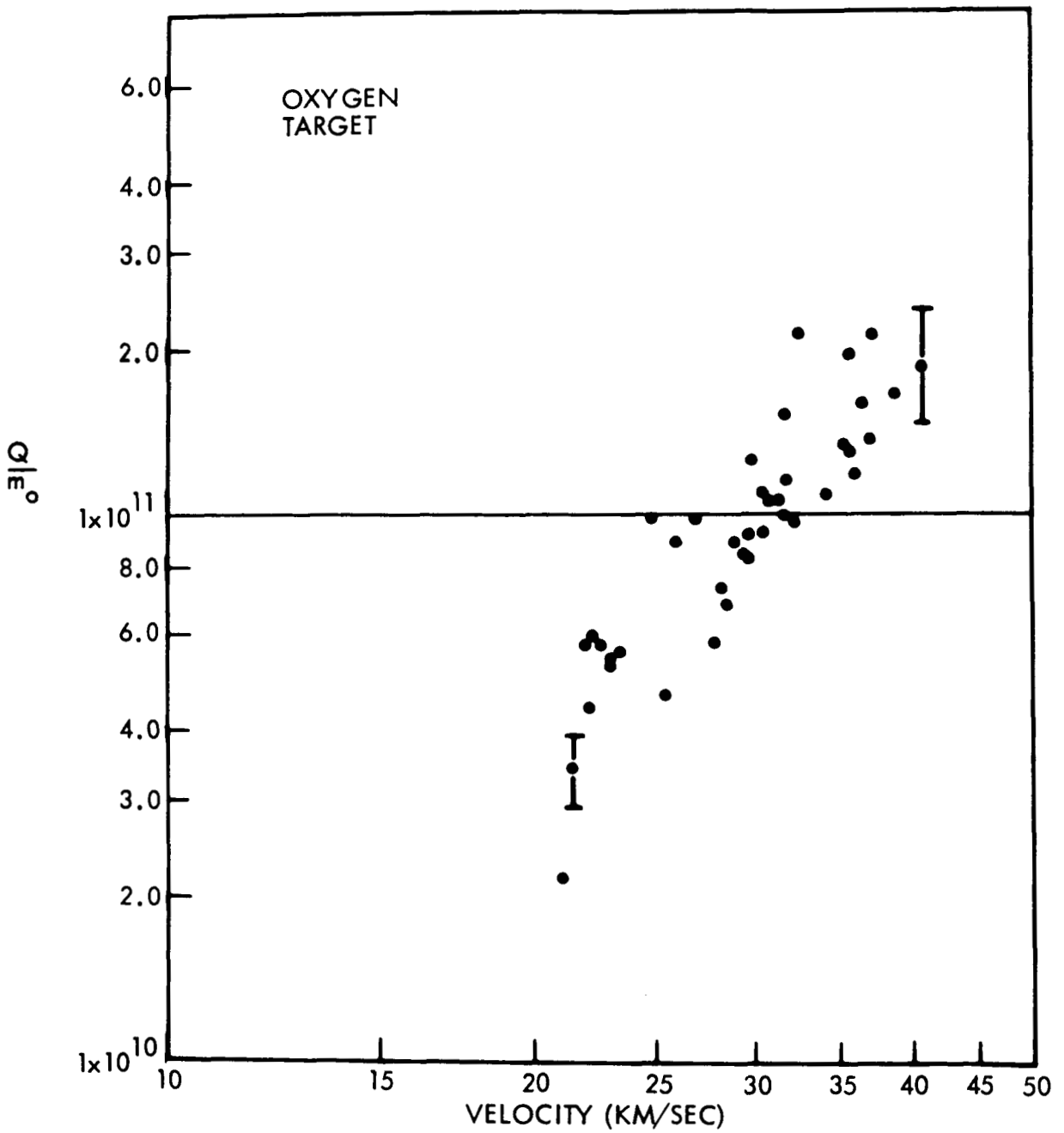

Figure 4. The quantity Q/m_o as a function of velocity for iron particles and an oxygen target gas. m_o is the particle mass and Q is the integrated current at the anode of an RCA 6199 PMT corrected for 100% light collection efficiency. The radiant sensitivity of the PMT was $7.8 \pm 1.8 \times 10^4$ amperes/joule. The error bars indicate the magnitude of the estimated random errors.

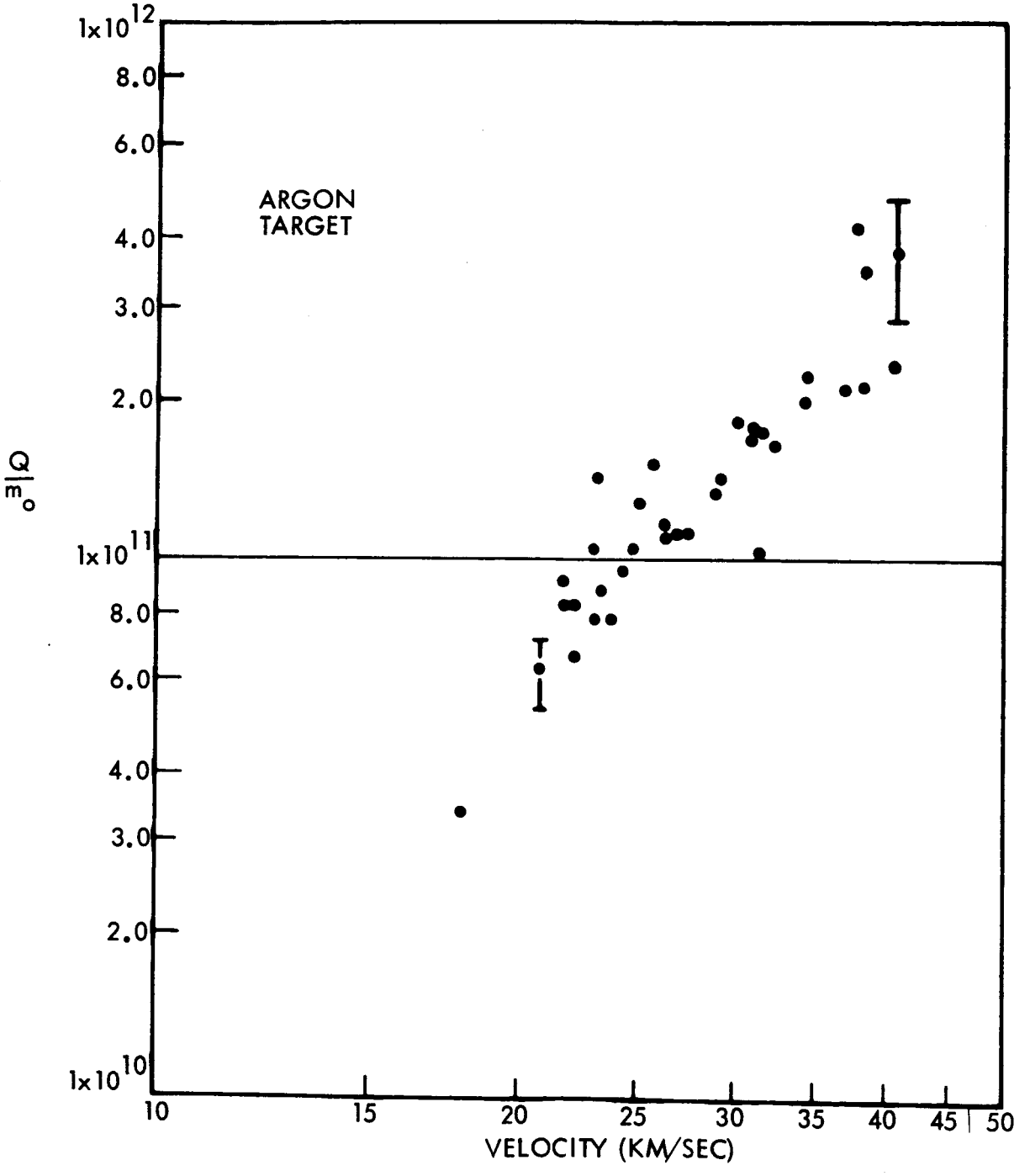

Figure 5. The quantity Q/m_o as a function of velocity for iron particles and an argon target gas. m_o is the particle mass and Q is the integrated current at the anode of an RCA 6199 PMT corrected for 100% light collection efficiency. The radiant sensitivity of the PMT was $7.8 \pm 1.8 \times 10^4$ amperes/joule. The error bars indicate the magnitude of the estimated random errors.

incident energy because of the spectral response characteristics of the PMT and the spectral distribution of radiation from the trail. The conversion of Q to a radiant energy measurement is discussed in succeeding sections of this paper. For the data given in Figures 2 through 5, Q was determined using an RCA 6199 photomultiplier tube with an S-11 spectral response. The measured sensitivity for monochromatic light at 4530 A was $7.8 \pm 1.8 \times 10^4$ coulombs/joule.

The dependence of Q/m_o on particle velocity appears to be quite similar for all of the target gases and the mean value of Q/m_o at a given particle velocity differs by no more than a factor of two for all of the gases. Q/m_o appears to be consistently greater for nitrogen than for oxygen at equal velocities. Within the scatter of the data points, the results obtained with air are consistent with this observation. The rate of change of Q/m_o with velocity appears to be smaller than predicted by contemporary meteor theory, at least for velocities above 20 km/sec. However, the three data points below 20 km/sec for the nitrogen gas target indicates that the velocity dependence may be stronger at low velocities.

The principal source of random error in these experiments is in the measurement of particle charge q, which directly affects the precision to which m_o is known. Typically, signal/noise ratios for signals from the charge detector range from about three to one at high particle velocities to better than ten to one at the low velocity extreme. The probable error in determining q ranges from an estimated $\pm$ 15% at high velocities to $\pm$ 5% at low velocities. Random errors in the measurement of v_o are probably less than $\pm$ 2% and the accelerating voltage is known to about $\pm$ 1%. This yields a random error in m_o of $\pm$ 20% at high velocities and about $\pm$ 10% at low velocities.

Possible systematic errors which effect the absolute accuracy of the particle mass measurement arise from the measurement of the input capacitance and gain of the preamplifier used with the charge detector, the absolute calibration of the Van de Graaff accelerating voltage, and the length of the velocity measurement range. It is estimated that the total systematic error in these quantities is less than $\pm$ 15%.

The absolute sensitivity of the main PMT was measured at 4630 A by the use of an Eppley spectral radiance standard in conjunction with a narrow pass-band interference filter. The estimated probable error in the measured absolute sensitivity is $\pm$ 16%. The main PMT was not calibrated in place nor was the orientation of the tube with respect to the earth's magnetic field the same in the calibration facility as it was in the experimental configuration. The PMT was magnetically shielded; nevertheless a probable error of $\pm$ 5% is assumed to be a reasonable estimate of variations in sensitivity due to orientation and location. The systematic error in the measurement of input capacitance and gain of the emitter-follower is estimated to be less than $\pm$ 2% which yields a total systematic error of $\pm$ 23% for the radiant energy measurement.

Although a stabilized high voltage power supply was used on the main PMT, the applied voltage was continuously monitored with a digital voltmeter. The maximum undetectable voltage variation was about $\pm$ 0.05% which results in a negligible variation in electron gain. The random error associated with reading the pulse amplitude from the photographic record of the PMT output signal is estimated to be $\pm$ 3%.

The other six PMT's were calibrated only on a relative basis using an un-filtered tungsten filament light source. All of these PMT's were set for equal radiant sensitivities by adjusting the voltage applied to the tubes. The PMT's all received their voltage from a common supply, but the total voltage applied to each tube was adjustable by means of potentiometers in series with the voltage-divider networks. The voltage at each photocathode was periodically checked with a digital voltmeter to check stability.

From the preceding discussion, the total estimated random error in determining Q/m_o ranges from about $\pm$ 23% at high velocities to $\pm$ 13% at low velocities. The random errors are due largely to the uncertainty in the value of m_o. The scatter of the data points shown in Figures 2 through 5 appears to be compatible with the estimated random errors although a few points show marked deviations. On the average, the scatter is somewhat greater than that observed in the ionizing efficiency experiments we have performed (see Ref. 7) which utilized essentially the same basic equipment

with similar estimated random errors. The slightly larger deviations may be attributable to some subtle pressure effect. However, there is not sufficient evidence available from these experiments to assess any systematic deviation due to variations in target gas pressure.

Assuming the spread in the data points is due solely to random errors, statistical averaging yields a value of Q/m_o good to $\pm$ 38% over the entire velocity range. The major uncertainty in the average value is due to the various systematic errors discussed above.

2.3 SPECTRAL CHARACTERISTICS OF THE LUMINOUS TRAIL

In the preceding section, the experimental results were expressed in terms of the quantity Q/m_o. In order to express this quantity in terms of radiant energy, the spectral distribution of the luminous source must be defined. Accordingly, a supplementary experiment designed to meet this objective was undertaken. This was accomplished by measuring the relative intensity in four narrow wavelength bands of a segment of the luminous trail. The experimental techniques were basically the same as those described previously; the only difference being in the target chamber assembly. RCA 6199 PMT's equipped with Optics Technology narrow pass-band filters were used as radiation detectors. The RC time constant at the PMT anodes was adjusted so that the amplitude of the output signal was proportional to the instantaneous intensity of the light source. The four PMT's were mounted with their axes perpendicular to the axis of the luminous trail and they viewed a segment of the trail $\sim$ 2 cm long. The relative sensitivities of the un-filtered PMT's were determined in place by measuring the relative signal amplitudes due to radiation from typical luminous trails. The relative sensitivities of the filter-PMT combinations were obtained by folding the known spectral transmission characteristics of the filters into the spectral response characteristic of the PMT's. We assumed a nominal S-11 response for each PMT. The areas under the resulting curves were taken as a measure of the sensitivity (when corrected for variations in electron gain); the full width at half maximum was $\sim$ 150 A. Further, it was assumed that the output signal from a given PMT was due to monochromatic radiation at the peak of the spectral response curve defined by the product of the filter and

S-11 spectral characteristics. The wavelengths chosen were 4040, 4350, 5320, and 5940 A.

Data were obtained for all the target gases over the full range of particle velocities. To within the accuracy of the experimental errors, no discernable differences in spectral shape were observed for the different target gases nor did the data exhibit an appreciable systematic variation with initial particle velocity. Accordingly, all the data for the N_2, O_2, and air targets were lumped together and the results are presented in Figure 6. Here we present the relative intensity of the luminous trail as a function of wavelength. The data were normalized to the point at 4040 A and the error bars are computed standard deviations for the ratio of signal amplitudes. The relatively large errors are attributed principally to statistical variations in signal amplitude due to very small signal levels observed with the filtered PMT's. Part of the variation might also be due to a systematic but small change of the spectrum with particle velocity. The line drawn through the points is a free hand straight-line fit to the data points and gives our best estimate of the spectral distribution of light from the luminous trail. It should be pointed out that the area under the curve is proportional to the total radiant energy and fairly large deviations in slope can be tolerated. For example, if one assumes an extreme case of constant light intensity at all wavelengths, the difference in areas under the curves would only be about 60%.

2.4 CALCULATION OF LUMINOUS EFFICIENCY

Assuming that the radiant energy at some wavelength λ_i is given by $E_{\lambda_i} = f(\lambda_i)\, E_o$ and that the sensitivity of the PMT at the same wavelength is given by $S_{\lambda_i} = g(\lambda_i)\, S_o$, the charge collected at the anode of the PMT due to radiation at λ_i is

$$Q_{\lambda_i} = f(\lambda_i)\, E_o \; g(\lambda_i)\, S_o \quad . \tag{4}$$

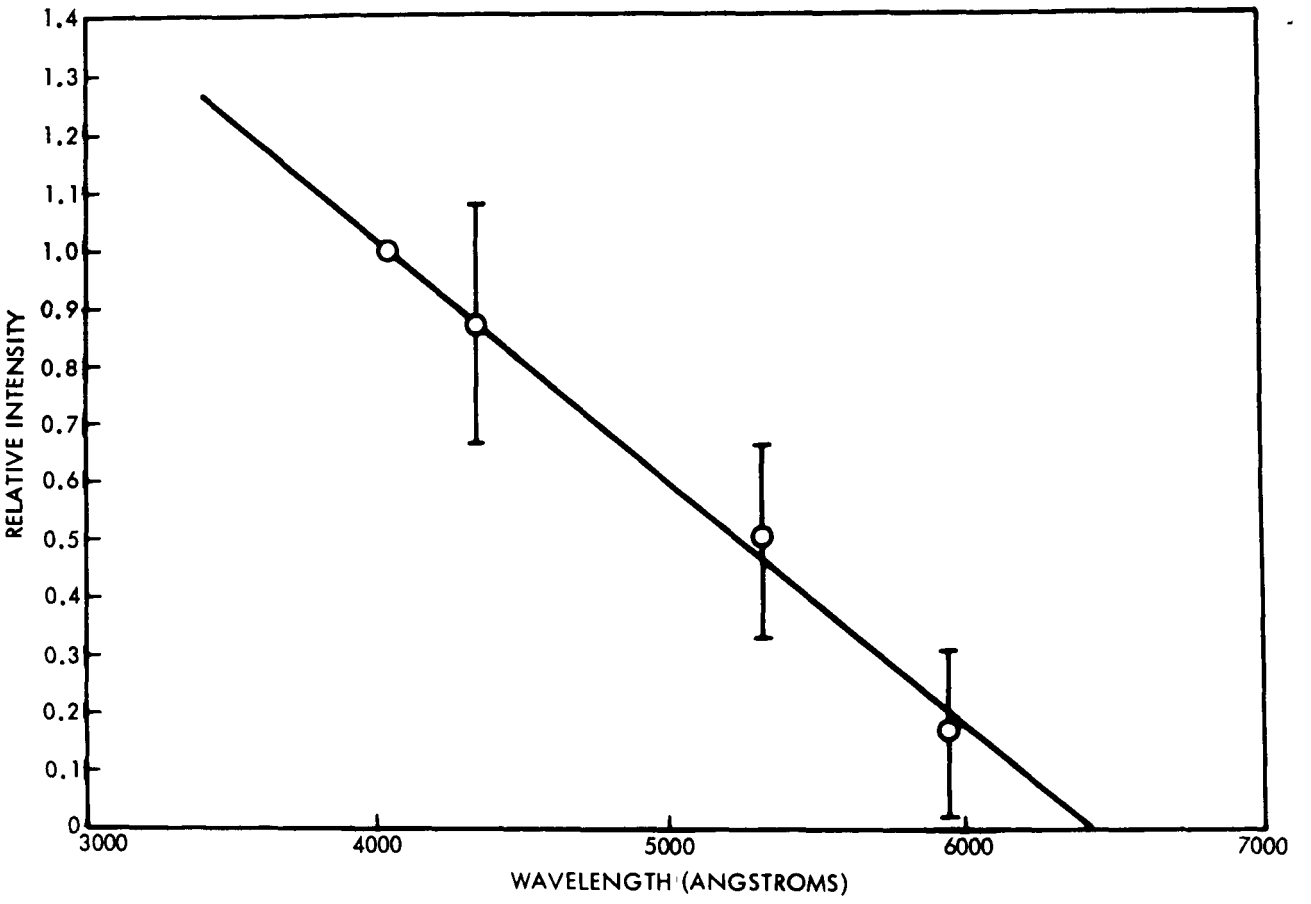

Figure 6. Spectral distribution of light from luminous trails. The intensity was determined at the indicated points and normalized to the point at 4040 A. Each point gives the average value for measurements conducted with target gases of nitrogen, oxygen, and air over the velocity range 20 - 40 km/sec. The error bars give the calculated standard deviations for each point.

Where $f(\lambda_i)$ is $f(\lambda)$ evaluated at λ_i and $g(\lambda_i)$ is $g(\lambda)$ also evaluated at λ_i, E_o is the radiant energy from the trail at some wavelength. S_o is the sensitivity of the PMT at a specified wavelength. Here $g(\lambda)$ corresponds to the S-11 spectral response characteristic of the PMT and $f(\lambda)$ is the spectral distribution of light from the trail as illustrated in Figure 6. The total charge at the anode due to radiation of all wavelengths is the integral of Eq. (4) over all wavelengths, i.e.,

$$Q = E_o S_o \int_\lambda g(\lambda) \quad f(\lambda)\, d\lambda \quad . \tag{5}$$

The total radiant energy from the trail is given by

$$E_x = E_o \int_\lambda f(\lambda)\, d\lambda \quad . \tag{6}$$

Eliminating E_o from these two equations and solving for E_x gives

$$E = \frac{Q}{S_o} \quad \frac{\int f(\lambda)\, d\lambda}{\int f(\lambda)\, g(\lambda)\, d} \quad . \tag{7}$$

This expression has been integrated graphically from 3400 A to 6300 A yielding for a final result

$$E_x = 1.54 \times 10^{-5}\, Q \quad \text{Joules} \quad , \tag{8}$$

for $S_o = 7.8 \times 10^4$ coulombs/joule at 4630 A.

Using this conversion factor, the air, N_2, and O_2 data are shown in Figures 7, 8, and 9 where the luminous efficiency τ_x as defined by

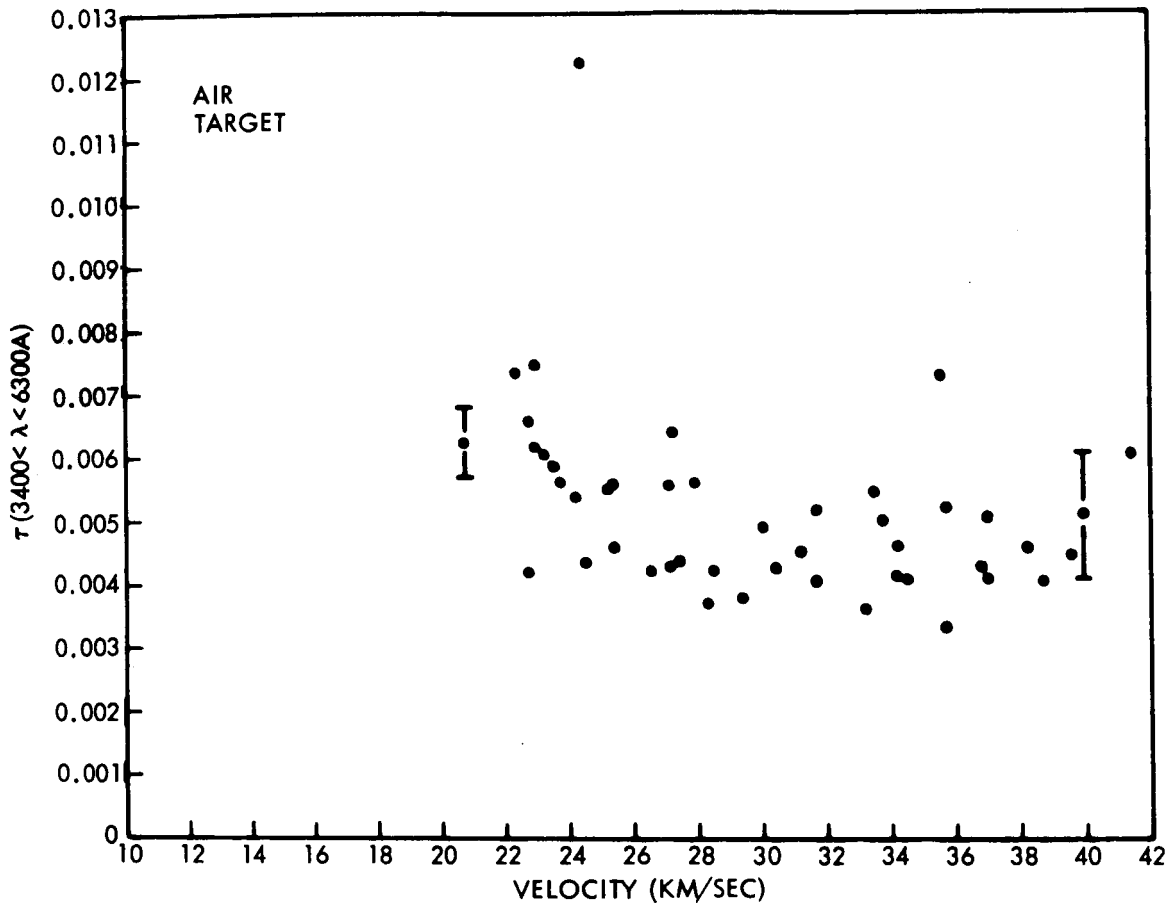

Figure 7. Luminous efficiency τ_x as a function of particle velocity for iron particles and an air target gas. The spectral range covered by the detector extends from 3400 to 6300 A. The magnitude of estimated random errors are shown on representative points.

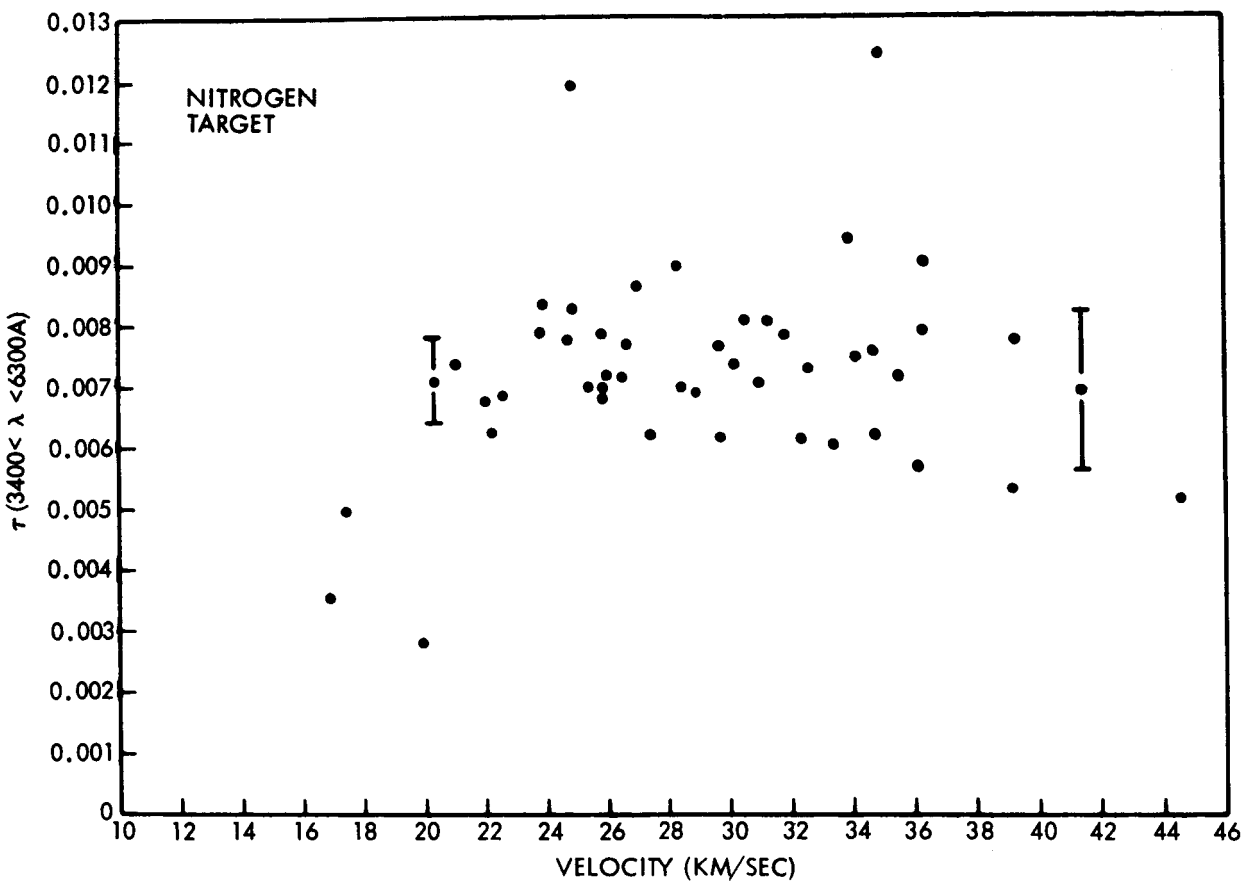

Figure 8. Luminous efficiency τ_x as a function of particle velocity for iron particles and a nitrogen target gas. The spectral range covered by the detector extends from 3400 to 6300 A. The magnitude of estimated random errors are shown on representative points.

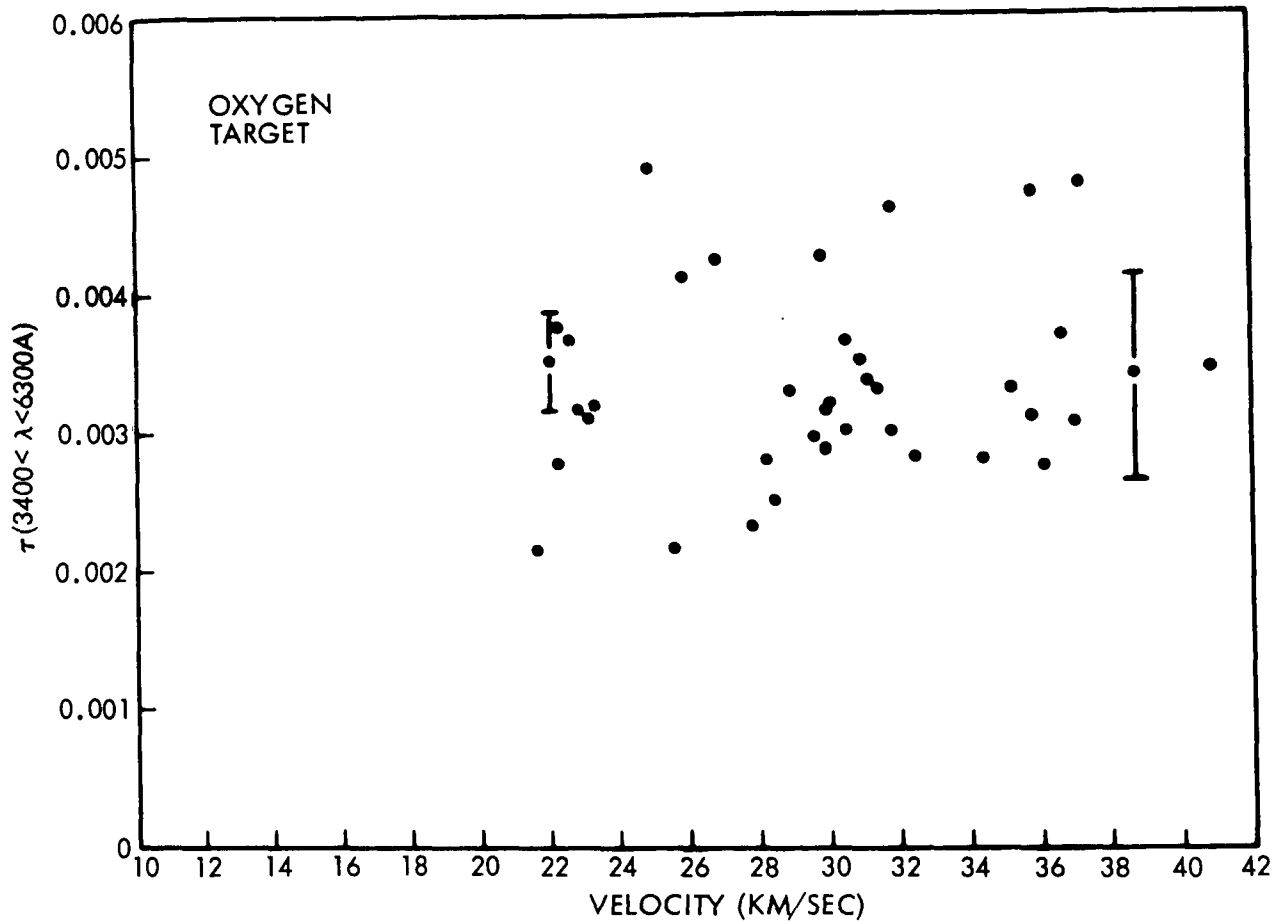

Figure 9. Luminous efficiency τ_x as a function of particle velocity for iron particles and an oxygen target gas. The spectral range covered by the detector extends from 3400 to 6300 A. The magnitude of estimated random errors are shown on representative points.

Eq. (2) is plotted as a function of particle velocity. The wavelength band to which these values of τ_x apply extends from 3400 to 6300 A.

Since the particle kinetic energy, equal to the product of particle charge and accelerating voltage, can be measured more precisely, the estimated random error in τ_x is only about $\pm$ 19% in contrast to an estimated uncertainty of $\pm$ 23% in Q/m_o. With the exception of a few isolated points, the scatter in the data appears to be consistent with the estimated uncertainties in the measured quantities. Systematic errors lead to an uncertainty in the average value of τ_x at a given velocity of perhaps $\pm$ 40% excluding systematic errors due to assuming the spectral distribution is not velocity dependent.

3. DISCUSSION OF RESULTS

A critical review of all of the attempts made to determine meteor luminous efficiency is beyond the scope of this report. For the sake of comparison, we arbitrarily accept the results of Verniani[5] as representative of contemporary work in this field. As discussed by Verniani, the results obtained from artificial meteors (particularly the work of McCrosky and Soberman[2]) are compatible with his results if a linear velocity dependence of τ_s is assumed. Our results, however, appear to support the results of Öpik's most recent analytical study.[1]

The most striking feature of our results is the fact that τ_x is nearly constant from about 20 to 40 km/sec for all of the target gases. Within the limits of the experimental errors, τ_x actually appears to decrease slightly with increasing velocity. This is in complete agreement with Öpik who predicted a slowly decreasing value of τ_v (luminous efficiency in the visual range) with velocity for meteors with greatly diluted comas. The dilution of the coma is a measure of the frequency of collisions between meteor atoms and a greatly diluted coma implies that collisions of this type produce negligible radiation. In other words, the radiation is due solely to collisions between meteor atoms and atmospheric molecules. Both qualitative arguments and a calculation of the dilution factor as suggested by

Öpik indicate that a greatly diluted coma is produced in our work.

In order to compare the results of our work with Öpik's on a quantitative basis, a conversion factor relating τ_v to the spectral range for which τ_x has been measured must be specified. A calculation made assuming the spectral distribution given in Figure 6 and assuming that the visual range extends from 4200 to 5800 A gives a conversion factor of ~ 2, i.e., Öpik's τ_v must be multiplied by a factor of two to take into account the wider spectral range used in these experiments. Using this factor, Öpik's result would predict values of $\tau_x = 0.002$ at 20 km/sec and $\tau_x = 0.001$ at 40 km/sec. These values are to be compared to the average measured value of $\tau_x = 0.005$. Thus, the theoretical and experimental results differ by a factor of two or three. This difference may not be excessive in view of the possible systematic experimental errors discussed above. Öpik does not assign a probable error to his values, but, in view of the complexity of the problem, the errors may be appreciable. Also, the value of the conversion factor used to obtain τ_x from τ_v is strongly dependent upon the spectrum of the luminous trail. For example, if the magnitude of the slope of the curve shown in Figure 6 is increased by 20% (which is within the range of experimental errors), the conversion factor becomes three rather than two. Another factor which might affect the results is the absolute target gas pressure. However, Öpik indicates that increasing the pressure (i.e., decreasing the collisional mean free path) would tend to lower the luminous efficiency. If pressure plays an important role, the discrepancy between experimental and theoretical values would likely be increased.

From his work, Verniani gives as a best estimate for cometary meteors $\tau_p = 5 \times 10^{-10} v$ where τ_p is the luminous efficiency in the photographic range and v is measured in cm/sec. The linear velocity dependence was obtained for both bright and faint meteors. To a first approximation $\tau_p = \tau_x$ and, therefore, no correction for different spectral response is required. It is generally assumed that only heavy elements (i.e., iron) contribute to excitation processes. According to Verniani, this yields the relationship $(\tau_p)_{Fe} \overset{\sim}{\sim} 6.5\ (\tau_p)_{cometary}$. From this, Verniani's results give $\tau_x = 0.0065$ at 20 km/sec and $\tau_x = 0.013$ at 40 km/sec. Unless the absolute gas pressure plays a significant and systematic role in our experiments, the agreement between our results and those of Verniani is not good, particularly with

respect to the velocity dependence. In terms of magnitudes, however, the disagreement is no worse than the discrepancy noted between our work and Öpik's predicted value.

A direct comparison between our results and those obtained by artificial meteor programs cannot be made because of the different velocity ranges. McCrosky and Soberman[2] give $\tau_p \simeq 0.004$ at 10 km/sec for a stainless steel artificial meteor. According to Öpik, the luminous efficiency does not decrease appreciably until the velocity falls below 10 km/sec. If this is the case, the results of McCrosky and Soberman may well be in agreement with our results.

4. CONCLUSIONS

The quantity luminous efficiency τ_x has been determined experimentally for microscopic iron particles at velocities ranging from 20 to 40 km/sec. It was found that τ_x is essentially independent of velocity over this range which is in agreement with Öpik's theory for meteors with greatly diluted comas. This result is in disagreement with the generally accepted viewpoint that τ_x increases linearly with velocity. The average value of τ_x over the spectral range from 3400 to 6300 A is 0.005 which is greater by about a factor of 2 or 3 than Öpik's value corrected for the different spectral ranges covered by his theory and our experiment. Considering the complexity of the theoretical problem and the estimated systematic errors of the experimental results, the results may well be in good agreement.

The most serious fundamental problem associated with interpreting the results of these experiments has to do with the absolute gas pressure. In our experiments the target gas pressure is significantly greater than for natural meteors. At present there is unsufficient data to observe a pressure affect if, indeed, such an effect exists. Future experiments will be undertaken to assess this problem.

Finally, we should point out that these results are applicable only to the greatly diluted coma case. For compact comas, Öpik predicts that

the luminous efficiency should increase with velocity. This effect is in general agreement with the linear velocity dependence for bright meteors assumed by most workers in the field and supported by Verniani's recent work.

REFERENCES

1. Ernst J. Öpik, Physics of Meteor Flight in the Atmosphere, Interscience Publishers, Inc., (New York), 1958.

2. R. E. McCrosky and R. K. Soberman, Smithsonian Contributions to Astrophysics, Vol. 7, p. 199 (1963).

3. W. O. Jewell and A. R. Wineman, "Preliminary Analysis of a Simulated Meteor Re-entry at 9.8 Kilometers Per Second", NASA Technical Note TN D-2268, April 1964.

4. W. G. Ayers, "Luminous Efficiency of an Artificial Meteor at 11.9 Kilometers Per Second", NASA Technical Note TN D-2931, August 1965.

5. F. Verniani, Smithsonian Contributions to Astrophysics, Vol. 8, p. 141 (1965).

6. M. F. Romig, AIAA Journal, Vol. 3, p. 385 (1965).

7. J. C. Slattery and J. F. Friichtenicht, "Ionization Probability of Iron Particles at Meteoric Velocities", to be published in the January, 1967 Astrophysical Journal.

8. J. F. Friichtenicht, Rev. Sci. Instr., Vol. 33, p. 209 (1962).

9. H. Shelton, C. D. Hendricks, Jr., and R. F. Wuerker, Journ. Appl. Phys., Vol. 31, p. 1243 (1960).

10. D. O. Hansen and N. L. Roy, Nucl. Instr. and Methods, Vol. 40, p. 209 (1966).